INTERNATIONAL JOURNAL OF NUMERICAL MODELLING: ELECTRONIC NETWORKS, DEVICES AND FIELDS
Int. J. Numer. Model. 2008; **21**:169–186
Published online 24 August 2007 in Wiley InterScience (www.interscience.wiley.com). DOI: 10.1002/jnm.651

Continuum modeling of large networks

Edwin K. P. Chong[1,*,†], Donald Estep[2] and Jan Hannig[3]

[1] *Department of Electrical and Computer Engineering, Colorado State University, Fort Collins, CO 80523, U.S.A.*
[2] *Department of Mathematics and Department of Statistics, Colorado State University, Fort Collins, CO 80523, U.S.A.*
[3] *Department of Statistics, Colorado State University, Fort Collins, CO 80523, U.S.A.*

SUMMARY

This paper is concerned with the modeling and simulation of extremely large networks. We derive a time-dependent diffusion–convection partial differential equation, the solution of which captures the global characteristics of a stochastic network model. Continuum modeling provides a powerful way to deal with the number of components in large networks and opens up the use of highly sophisticated mathematical tools such as adaptive finite element methods. This, in turn, makes it possible to carry out—with reasonable computational burden even for very large systems—network performance evaluation and prototyping, network design, systematic parameter studies, and optimization of network characteristics.

Received 9 May 2007; Accepted 18 June 2007

KEY WORDS: continuum modeling of networks; large network modeling; network optimization; nonlinear parabolic problems; wireless *ad hoc* networks

1. INTRODUCTION

This paper is concerned with the modeling and simulation of networks involving a large number of nodes using time-dependent partial differential equations (PDEs). The analysis and design of large networks is a critically important engineering problem impacting a number of fields. In many applications, numerical simulation is the tool of choice for the design and evaluation of

*Correspondence to: Edwin K. P. Chong, Department of Electrical and Computer Engineering, Colorado State University, Fort Collins, CO 80523, U.S.A.
† E-mail: edwin.chong@colostate.edu

Contract/grant sponsor: National Science Foundation; contract/grant numbers: ECCS-0700559, DMS-0107832, DGE-0221595003, MSPA-CSE-0434354, DMS-0707037, DMS-0504737
Contract/grant sponsor: Department of Energy; contract/grant numbers: DE-FG02-04ER25620, DE-FG02-05ER25699
Contract/grant sponsor: National Aeronautics and Space Administration; contract/grant number: NNG04GH63G
Contract/grant sponsor: Sandia Corporation; contract/grant number: PO299784

large networks. However, the computational overhead associated with direct simulation severely limits the size and complexity of networks that can be studied in this fashion. Performing numerical simulations of large stochastic networks has been widely recognized as a major hurdle to future progress in understanding and evaluating large networks.

In this paper, we demonstrate that important global characteristics (what might be called 'macroflow behavior') of very large networks can be captured by a continuum model posed in terms of a PDE. The continuum model considers the behavior of the components on the scale of the aggregate rather than of the individual, while the individual characteristics of the components enter the model through the form of the equations and the parameters defining the model. Continuum modeling of large networks by PDEs provides a powerful way to deal with the number of components in large networks and opens up the use of highly sophisticated mathematical tools such as adaptive finite element methods. This, in turn, makes it possible to carry out network performance evaluation and prototyping, network design, systematic parameter studies, and optimization of network characteristics with reasonable computational burden even for very large systems.

It turns out that the physical characteristics of a network significantly affect the derivation of the continuum model. In order to focus ideas, we consider an ideal network that represents important characteristics of both wireless *ad hoc* networks and remote sensing networks.

Interest in wireless *ad hoc* networks has flourished in recent years. At the same time, the analysis of such networks has proven to be challenging. A particular line of research focuses on deriving scaling laws in an asymptotic regime of behavior. For example, a seminal paper by Gupta and Kumar [1] shows that under certain modeling assumptions, it is possible to characterize the scaling law of the transport capacity in the asymptotic regime, where the number of nodes N grows to infinity. Roughly, they show that the throughput grows as $O(\sqrt{N})$. This result has spawned numerous papers that characterize asymptotic scaling laws for wireless networks in different settings (e.g. [2–4]). Despite the ground-breaking nature of these scaling-law results, they do not provide any means to determine the *actual* throughput of a network with, say, a million nodes. Simulation remains the only method of answering such questions. However, simulation tools do not currently support very large network sizes.

The possibility of networking, not only computers and communication devices but also sensors, has led to a significant current interest in sensor networks (see, e.g. NSF's Sensors and Sensor Networks Program [5]). Similarly to *ad hoc* networks, sensor networks consist of sensors connected together *via* wireless links. However, sensor networks exhibit some unique features, including limitations in energy, bandwidth, and processing power. Analysis of such networks has closely followed that of wireless *ad hoc* networks, characterizing asymptotic scaling laws as the number of sensors grows (e.g. [6, 7]). The performance of large-scale sensor networks is still not possible with state-of-the-art simulators.

2. A DISCRETE STOCHASTIC NETWORK MODEL

We consider a network of wireless nodes distributed uniformly over a domain that represents an idealized network of sensors that continuously generate data, which need to be communicated to destination nodes located on the edge of the network. We illustrate a two-dimensional model in Figure 1. These destination nodes may represent, for example, communication relay devices that transmit the sensor data to a satellite.

DOI: 10.1002/jnm

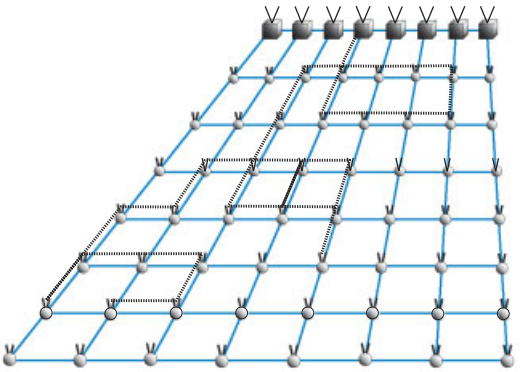

Figure 1. An illustration of a network consisting of a set of wireless nodes distributed uniformly over a rectangular grid. A set of receivers is located at the far edge. We show the possible path of a message originating from a node located in the left-front region.

The derivation of a PDE model starts with a detailed stochastic model for the transmission of information in the network. The network consists of N wireless nodes, each capable of either receiving or transmitting messages from or to its *immediate* neighbors. This is a simplification of a more realistic model using a power law to model the range of transmission, but this allows for a relatively simple presentation. At each time instant $k = 0, 1, \ldots$, we assume that a message is generated in a random fashion at each node and each node probabilistically decides to transmit or receive, but not both. Each node has the capacity to store messages in a *queue*. On the outer boundary of the network region, we place special nodes that can only receive messages. These nodes represent specialized devices that collect data from the network of sensors. The basic goal is for the messages in the network to be routed to these special edge nodes. There are many possible routing schemes, but all have to take into account the fact that the communication is interference-limited because all nodes share the same wireless channel.

We derive a model for a particular communication scheme. At each time instant, each node decides to be a sender (independent of others) with probability depending on the (expected) number of messages in its queue, i.e. the probability that the node at n is trying to send a message at time k is $F(n, Q(k, n))$, where Q is the expected queue length and F is a given function. The node then probabilistically chooses one of its neighbors in an attempt to transmit a message independent of the choices made by its neighbors. The transmission is successful if there is no interference, i.e. the intended receiver and its other neighbors are not trying to transmit messages of their own. Additionally, at each time instant, node n generates messages and adds them to its queue. We assume that the number of messages generated at node n follows a Poisson distribution with mean $G(n)$. This assumption is consistent with assuming that the messages are arriving at node n in a homogeneous random fashion.

This description gives rise to a recurrent relation for the length of the queue at time k and at node position n. The sequence of queue-length vectors $\{[\tilde{Q}(k, 1), \ldots, \tilde{Q}(k, N)]\}$ forms a Markov process.

DOI: 10.1002/jnm

The specialized receiver nodes at the edge of the network obey a different set of rules. The protocols employed by the specialized receiver nodes give rise to boundary conditions for the PDE model, with the specific conditions depending on the protocols that govern its behavior. We consider three types of boundary behaviors:

- A *sink* is a receiver that receives *all* the messages passed to it (and then passes them on to the final user). A sink never transmits anything into the network.
- A *wall* is a boundary node that returns all the messages passed to it back into the system. In other words, it is not a 'consumer' of messages. We assume that messages encounter the same interference coming into a wall as in the regular system.
- A *semi-permeating wall* is a compromise between a wall and a sink. It receives messages, stores them in a queue, and returns them back to the system in a similar manner as a regular node. Additionally, it removes messages from its queue and passes them to the final user with some probability $S(n, Q(k, n))$.

3. A CONTINUUM MODEL IN ONE DIMENSION

The goal is to construct a PDE model that describes the limiting mean behavior of the system as the number of nodes grows to infinity. In the first case, we assume that the network is one dimensional in the sense that the nodes are uniformly located at N integer positions on the line. At the edge of the network, nodes $n = 0$ and $n = N + 1$, we place two special nodes that can only receive messages. The basic goal is to route the messages in the network to these two special edge nodes taking into account the interference caused by sharing the wireless channel.

In this case, each node chooses one of its two neighbors to transmit a message. We denote the probabilities of sending to the right and left by $P_r(n)$ and $P_l(n)$ with $P_r(n)+P_l(n) = 1$. The Markov process of queue-length vectors $\{[\tilde{Q}(k, 1), \ldots, \tilde{Q}(k, n)]\}$ has the transition rule:

$$\tilde{Q}(k+1,n) = \begin{cases} \tilde{Q}(k,n) + 1 + \tilde{G}(n,k) \quad \text{with probability} \\ [1 - F(n, Q(k,n))] \\ \times[P_r(n-1)F(n-1, Q(k,n-1))(1 - F(n+1, Q(k,n+1))) \\ +P_l(n+1)F(n+1, Q(k,n+1))(1 - F(n-1, Q(k,n-1)))] \\ \tilde{Q}(k,n) - 1 + \tilde{G}(n,k) \quad \text{with probability} \\ F(n, Q(k,n)) \\ \times[P_r(n)(1 - F(n+1, Q(k,n+1)))(1 - F(n+2, Q(k,n+2))) \\ +P_l(n)(1 - F(n-1, Q(k,n-1)))(1 - F(n-2, Q(k,n-2)))] \\ \tilde{Q}(k,n) + \tilde{G}(n,k) \quad \text{otherwise} \end{cases} \tag{1}$$

Here $\tilde{G}(n, k)$, $k = 1, \ldots$ are independent Poisson random variables with mean $G(n)$. Taking an expectation and simplifying, we obtain the following difference equation for the mean

DOI: 10.1002/jnm

queue length:

$$\begin{aligned} Q(k+1,n) - Q(k,n) = {} & [1 - F(n, Q(k,n))] \\ & \times [P_r(n-1)F(n-1, Q(k,n-1))(1 - F(n+1, Q(k,n+1))) \\ & + P_l(n+1)F(n+1, Q(k,n+1))(1 - F(n-1, Q(k,n-1)))] \\ & - F(n, Q(k,n)) \\ & \times [P_r(n)(1 - F(n+1, Q(k,n+1)))(1 - F(n+2, Q(k,n+2))) \\ & + P_l(n)(1 - F(n-1, Q(k,n-1)))(1 - F(n-2, Q(k,n-2)))] \\ & + G(n) \end{aligned} \tag{2}$$

We now take an asymptotic limit of this difference equation to obtain an approximating PDE. Generally, this requires an *a priori* assumption about how the space and time scales are related. We scale time and space in such a way that the location of two neighboring nodes and times differ by $\mathrm{d}x$ and $\mathrm{d}t$, respectively, i.e. $x = x_0 + n\,\mathrm{d}x$ and $t = t_0 + k\,\mathrm{d}t$ for some fixed spatial and temporal reference points x_0 and t_0, respectively. We assume $\mathrm{d}t = \mathrm{d}x^2$, which is sometimes called the hydrodynamic scaling of time and space. The communication protocol we pose above describes random forwarding of messages between neighboring nodes and is nominally a diffuse process. The hydrodynamic scaling is natural for diffusion processes. For the variables obtained in the limit of $\mathrm{d}t,\ \mathrm{d}x \to 0$, we use lower-case notation, so that $q(t,x)$ corresponds to $Q(k,n)$, and $f(x, q(t,x))$ corresponds to $F(n, Q(k,n))$. Assuming that the solution of the limiting partial differential equation is smooth, we can write

$$\begin{aligned} q(t + \mathrm{d}t, x) &= q(t,x) + \frac{\partial}{\partial t} q(t,x)\,\mathrm{d}t + \mathbf{o}(\mathrm{d}t) \\ q(t, x + \mathrm{d}x) &= q(t,x) + \frac{\partial}{\partial x} q(t,x)\,\mathrm{d}x + \frac{\partial^2}{\partial x^2} q(t,x)\frac{\mathrm{d}x^2}{2} + \mathbf{o}(\mathrm{d}x^2) \end{aligned} \tag{3}$$

We substitute these expansions into the scaled difference equation, divide both sides of the equation by $\mathrm{d}x^2$, and take the limit as $\mathrm{d}x \to 0$.

To ensure a finite non-degenerate limit, we assume that

$$P_r(n) = \tfrac{1}{2} + c_r(x, q, q')\,\mathrm{d}x, \quad P_l(n) = \tfrac{1}{2} + c_l(x, q, q')\,\mathrm{d}x, \quad G(n) = g(x)\,\mathrm{d}t \tag{4}$$

where $q' = \partial q / \partial x$. This assumption is not merely a matter of technical convenience—it also has some important practical significance. For example, $G(n) = g(x)\,\mathrm{d}t$ guarantees that the number of messages entering the system from outside over finite time intervals remains finite throughout the limiting process. Similarly, the probabilities P_r and P_l are introducing a directional bias in the system. The assumption in (4) ensures that this directional bias remains finite over a finite interval. For technical reasons, we also assume that the functions f, c_r, c_l, and g are smooth, and, in addition, f is twice differentiable, monotone, and takes values between 0 and 1 with $f(0) = 0$. Further conditions on f, c_r, and c_l might be required to guarantee that the model PDE has smooth solutions. In the simulations in this paper, we assume that $f(x,q) = q$.

DOI: 10.1002/jnm

This argument leads to the following limiting differential equation:

$$\frac{\partial q(t,x)}{\partial t} = \frac{\partial}{\partial x}\left(\frac{1}{2}(1-f(x,q(t,x)))(1+3f(x,q(t,x)))\frac{\partial}{\partial x}f(x,q(t,x))\right) + \frac{\partial}{\partial x}((c_l(x,q,q')-c_r(x,q,q'))f(x,q(t,x))(1-f(x,q(t,x)))^2) + g(x) \tag{5}$$

3.1. Boundary conditions

We derive boundary conditions for the three types of boundary nodes.

Consider a sink at the right-hand node, which never transmits into the network. The node just to the right of the sink therefore receives messages only from the right. Also, when that node transmits to the right, there is no interference. This leads to the difference equation,

$$\begin{aligned} Q(k+1,n)-Q(k,n) = {} & [1-F(n,Q(k,n))]P_r(n-1)F(n-1,Q(k,n-1)) \\ & - F(n,Q(k,n))[P_r(n)+P_l(n)(1-F(n-1,Q(k,n-1)))] \\ & \times (1-F(n-2,Q(k,n-2)))] \end{aligned}$$

If we rescale as before and take a limit, we arrive at the homogeneous Dirichlet boundary condition at the sink, i.e. $q(x,t)=0$. The same condition is derived analogously for a sink on the left.

For a wall, we assume the same interference coming into the wall as in the regular system. This yields the following difference equation for a wall located at the right end of the domain:

$$\begin{aligned} Q(k+1,n)-Q(k,n) = {} & [1-F(n,Q(k,n))] \\ & \times [P_r(n-1)F(n-1,Q(k,n-1))(1-F(n+1,Q(k,n+1))) \\ & - F(n,Q(k,n)) \\ & \times [P_l(n)(1-F(n-1,Q(k,n-1)))(1-F(n-2,Q(k,n-2)))] \end{aligned}$$

Rescaling as before and taking a limit, we arrive at the homogeneous Neumann boundary condition at the wall:

$$\frac{1}{2}(1-f(x,q(t,x)))(1+3f(x,q(t,x)))\frac{\partial}{\partial x}f(x,q(t,x)) + (c_l(x,q,q')-c_r(x,q,q'))f(x,q(t,x))(1-f(x,q(t,x))^2 = 0$$

The same condition is derived analogously if the wall is at the left side.

Finally, for a semi-permeating wall, we assume that the same interference coming into the wall as in the regular system. This leads to the following difference equation for a

DOI: 10.1002/jnm

semi-permeating wall located at the right end of the domain:

$$\begin{aligned} Q(k+1,n) - Q(k,n) = {} & [1 - F(n, Q(k,n))] \\ & \times [P_r(n-1)F(n-1, Q(k,n-1))(1 - F(n+1, Q(k,n+1))) \\ & - F(n, Q(k,n)) \\ & \times [P_l(n)(1 - F(n-1, Q(k,n-1)))(1 - F(n-2, Q(k,n-2)))] \\ & - S(n, Q(k,n)) \end{aligned}$$

Assuming that $S(n, Q(k,n)) = s(x, q(t,x))\,\mathrm{d}x$, we obtain the following boundary condition:

$$\begin{aligned} & \frac{1}{2}(1 - f(x, q(t,x)))(1 + 3f(x, q(t,x)))\frac{\partial}{\partial x} f(x, q(t,x)) \\ & + (c_l(x,q,q') - c_r(x,q,q'))f(x, q(t,x))(1 - f(x, q(t,x)))^2 = -s(x, q(t,x)) \end{aligned}$$

The analogous argument at the left end of the domain yields

$$\begin{aligned} & \frac{1}{2}(1 - f(x, q(t,x)))(1 + 3f(x, q(t,x)))\frac{\partial}{\partial x} f(x, q(t,x)) \\ & + (c_l(x,q,q') - c_r(x,q,q'))f(x, q(t,x))(1 - f(x, q(t,x)))^2 = s(x, q(t,x)) \end{aligned}$$

Note that if $S(n, Q(k,n)) = \mathbf{o}(\mathrm{d}x)$, we get a Neumann zero condition and the receiver behaves like a wall. On the other hand, if $1/S(n, Q(k,n)) = \mathbf{o}(1/\mathrm{d}x)$, we get a Dirichlet zero condition and the receiver behaves asymptotically like a sink.

3.2. Conclusion and characteristics of the PDE model

We summarize the derivation with the following theorem.

Theorem
If the solution q of the PDE model (5) together with appropriate boundary conditions is sufficiently smooth, then q satisfies the difference equation for the mean queue length (2) to order $\mathbf{o}(\mathrm{d}t) = \mathbf{o}(\mathrm{d}x^2)$ at each node of the discrete network.

As we consider denser and denser networks, this approximation holds at a denser set of points in the network domain.

The PDE model (5) is a quasi-linear diffusion–convection–reaction problem. The diffusion coefficient $\frac{1}{2}(1 - f(x, q(t,x)))(1 + 3f(x, q(t,x)))$ is positive unless $f = 1$ at some point, in which case it becomes a singular problem. Our numerical investigations suggest that this problem is diffusion dominated for a reasonable range of the coefficient $(c_l(x,q,q') - c_r(x,q,q'))$ and the solutions are smooth. The coefficient $(c_l(x,q,q') - c_r(x,q,q'))$ represents the bias in routing messages toward one direction or the other by adding *convection* to the PDE. In general, we can expect that the difficulty in finding solutions depends critically on the size of the convection coefficient. As this becomes larger, the problem becomes more difficult to solve as illustrated below.

In general, we cannot expect to find closed-form solutions of (5). Moreover, such characteristics as highly localized forcing functions, convection, various boundary conditions, and the possibility of boundary layers, make finding numerical solutions nontrivial. We use sophisticated adaptive finite element methods in the simulations below.

DOI: 10.1002/jnm

3.3. Numerical comparisons

To illustrate the approximation properties of the PDE model, we compare Monte Carlo simulations of the original discrete network model with the numerical solution of the PDE model. For the discrete network, we place the nodes $x_n = 20n/(N+1) - 10$, $n = 1, \ldots, N$, uniformly on the domain $[-10, 10]$ and the special boundary nodes ($n = 0$ and $n = N+1$) at locations -10 and 10, respectively.

For convenience, we normalize the queue-length variables by a constant maximum queue size $Q_{\max} = 20$, so that the dependent variables $Q(k,n)$ and $q(t,x)$ lie between 0 and 1. In the comparison, we use $c_l(x,q,q') - c_r(x,q,q') = c$ and $f(x,q) = q$. The equation $f(x,q) = q$ represents the transmission rule where a node transmits a message with a probability proportional to its mean queue length. In practice, we may approximate this rule by making this probability proportional to the *instantaneous* queue length. This approximation is justified if the variance of the instantaneous queue length is small relative to the mean queue length. As we will see later, this turns out to be the case in practice, which means that the approximation has little impact on the accuracy of the PDE model compared with the actual network behavior.

For the particulars given above, the PDE simplifies to

$$\frac{\partial q(t,x)}{\partial t} = \frac{\partial}{\partial x}\left(\frac{1}{2}(1+3q(t,x))(1-q(t,x))\frac{\partial q(t,x)}{\partial x}\right) + \frac{\partial}{\partial x}(cq(t,x)(1-q(t,x))^2) + g(x)$$

The PDE is defined on the domain $(-10, 10)$, with boundaries at -10 and 10. We considered two boundary conditions: the sink $q(t,x) = 0$ and the wall

$$\frac{\partial}{\partial x} q(t,x) = -\frac{2cq(t,x)(1-q(t,x))}{1+3q(t,x)}$$

We use the initial condition $q(0,x) = 10^{-2}\sqrt{(2/\pi)}\mathrm{e}^{-x^2}$ so that initially the nodes in the middle have messages to transmit, while those near the boundaries have none. We also add messages to the system with the rate $g(x) = l\sqrt{(2/\pi)}\mathrm{e}^{-x^2}$, where $l > 0$ is a parameter determining the total load of the system.

We compare simulations of the stochastic network model with $N = 51$ nodes along with numerical solutions of the PDE model in Figures 2 and 3. In practice, we do not know the average queue size Q needed in (1) so we simulate the stochastic network using two approaches for computing the probability of transmission. In the first, we choose Q to be the average over an ensemble of 400 repeated simulations. In the second, we approximate the rule involving f using the instantaneous queue length $\tilde{Q}$. Note that $\tilde{Q}$ is an unbiased estimator of Q.

In the first three simulations shown in Figure 2, we place sinks at the boundaries and vary the convection. The first has no convection ($c = 0$), the second has a moderate convection of $c = 25$, and the third has a relatively large convection of $c = 100$. The solutions become increasingly nonsymmetric as a result of the convection increasing. Yet, the PDE solution remains very accurate for all three simulations.

In the fourth simulation shown in Figure 3, we place walls (instead of sinks) at the boundaries and use a convection of $c = 100$. The discrete simulation becomes unstable as the messages can no longer be transmitted through the boundaries sufficiently rapidly to keep the queues from becoming full. Remarkably, the PDE model appears to still capture some crude mean behavior.

DOI: 10.1002/jnm

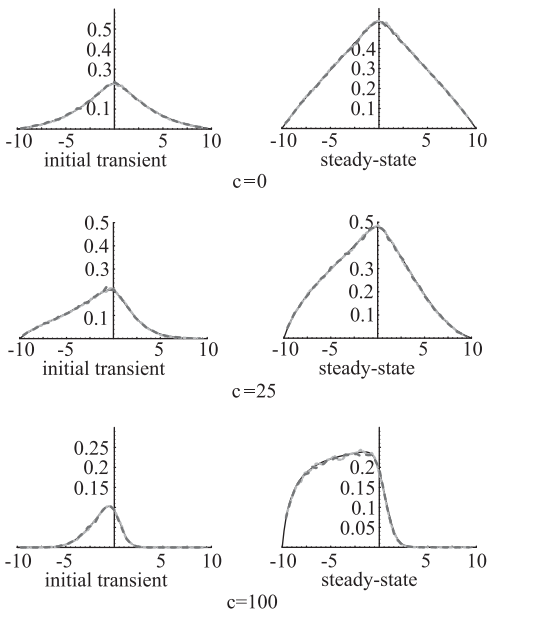

Figure 2. Simulations of the one-dimensional models with sink boundary conditions. From top to bottom, the convection c is 0, 25, and 100.

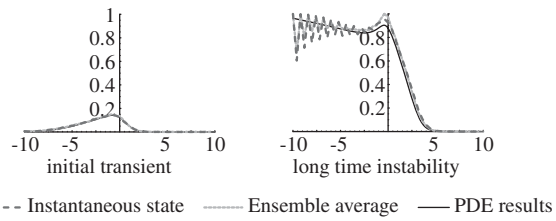

Figure 3. Simulation results for the one-dimensional model with wall boundary conditions and $c = 100$.

In most cases, it is difficult to distinguish between the PDE results and the two approaches to the stochastic network simulation, which is an indication of the strong agreement among them. We stress that the numerical solution of the PDE model takes a negligible amount of computer time compared with running discrete Monte Carlo simulations. Simulation times are fractions of a second to time on the order of hours.

4. MODELING IN HIGHER SPATIAL DIMENSIONS

The extension of the modeling approach to higher dimensions is straightforward, though the calculations are more tedious. The resulting PDE is again a quasilinear diffusion–convection–

DOI: 10.1002/jnm

reaction problem. We describe the model for a two-dimensional network, omitting some of the more onerous details. Note that higher dimensions lead to a number of interesting issues because the geometry now becomes an important consideration. For example, we now can route messages in such a way as to avoid areas that might be prone to develop congestion. This means that we have to deal with the spatial structure of the strategy that is used to describe the communication in the network.

4.1. The model in two dimensions

We now denote the mean queue length at time k by $Q(k,n,m)$ at node location (n,m), where we switch to a two-dimensional node numbering scheme. The associated probability of being a sender is therefore $F(n,m,Q(k,n,m))$. We denote the corresponding continuous limiting variables by $q(t,x,y)$ and $f(x,y,q)$, where the variables x, y, and t are related to n, m, and k, respectively, through scaling. The biases in message-routing probabilities are

$$P_{\mathrm{n}}(n,m) = \tfrac{1}{4} + c_{\mathrm{n}}(x,y,q,\nabla q)\,\mathrm{d}y, \quad P_{\mathrm{e}}(n,m) = \tfrac{1}{4} + c_{\mathrm{e}}(x,y,q,\nabla q)\,\mathrm{d}x$$
$$P_{\mathrm{s}}(n,m) = \tfrac{1}{4} + c_{\mathrm{s}}(x,y,q,\nabla q)\,\mathrm{d}y, \quad P_{\mathrm{w}}(n,m) = \tfrac{1}{4} + c_{\mathrm{w}}(x,y,q,\nabla q)\,\mathrm{d}x$$

for north, east, south, and west directions, respectively. The limiting PDE is

$$\begin{aligned}\frac{\partial q}{\partial t} = \nabla \cdot \Bigg(& \frac{1}{4}(1-f(x,y,q))^3(1+5f(x,y,q))\nabla f(x,y,q) \\ & + \begin{pmatrix} c_{\mathrm{w}}(x,y,q,\nabla q) - c_{\mathrm{e}}(x,y,q,\nabla q) \\ c_{\mathrm{s}}(x,y,q,\nabla q) - c_{\mathrm{n}}(x,y,q,\nabla q) \end{pmatrix} f(x,y,q,\nabla q)(1-f(x,y,q,\nabla q))^4 \Bigg) \\ & + g(x,y) \end{aligned} \tag{6}$$

We can also derive boundary conditions that correspond to three types of boundary nodes. Specifically, a sink boundary corresponds to an outlet—it removes all the messages that reach it from the system, leading to the homogeneous Dirichlet condition $q(t,x,y) = 0$. A wall corresponds to the boundary where there is no outlet—it returns all the messages back to the system. This leads to the homogeneous Neumann condition. To be precise, let $\mathbf{t}$ be the normal unit vector pointing toward the interior of the domain. Then, the condition is

$$\begin{aligned} 0 = \mathbf{t} \cdot \Bigg(& \frac{1}{4}(1-f(x,y,q(t,x,y)))^3(1+5f(x,y,q(t,x,y)))\nabla f(x,y,q(t,x,y)) \\ & + \begin{pmatrix} c_{\mathrm{w}}(x,y,q,\nabla q) - c_{\mathrm{e}}(x,y,q,\nabla q) \\ c_{\mathrm{s}}(x,y,q,\nabla q) - c_{\mathrm{n}}(x,y,q,\nabla q) \end{pmatrix} f(x,y,q(t,x,y))(1-f(x,y,q(t,x,y)))^4 \Bigg) \end{aligned}$$

Finally, a semi-permeating wall removes messages from the system with probability $S(n,m,Q)$. Assuming that $S(n,m,Q) = s(x,y,q)\,\mathrm{d}x$, this boundary-node behavior leads to the following

DOI: 10.1002/jnm

boundary condition: using the notation $\mathbf{t}$ as before,

$$s(x,y,q) = \mathbf{t} \cdot \left(\frac{1}{4}(1-f(x,y,q))^3(1+5f(x,y,q))\nabla f(x,y,q) + \begin{pmatrix} c_w(x,y,q,\nabla q) - c_e(x,y,q,\nabla q) \\ c_s(x,y,q,\nabla q) - c_n(x,y,q,\nabla q) \end{pmatrix} f(x,y,q)(1-f(x,y,q))^4 \right)$$

Theorem
If the solution q of the PDE model (6) together with appropriate boundary conditions is sufficiently smooth, then q satisfies the difference equation for the mean queue length to order $\mathbf{o}(\mathrm{d}t) = \mathbf{o}(\mathrm{d}x^2)$ at each node of the discrete network.

4.2. Numerical comparisons

We present some simulation results for a two-dimensional system. The discrete network consists of 83×83 nodes with a maximum queue size of $Q_{\max} = 100$, laid out as a grid on the square $[-1,1] \times [-1,1]$. We choose $f = q$, $c_n = c_w = c_s = c_e = 0$,

$$g(x,y) = 0.4 \times \mathrm{e}^{-2x^2-2y^2}/1.4311$$

and sink conditions at all four boundaries. We use 200 simulations to compute the ensemble average. The computational time needed to simulate the discrete network until it reaches steady state is 10 days, while the PDE solved on the same machine takes less than a second. We could not simulate any larger discrete networks.

In Figure 4, we show a snap shot of the contours of the discrete and continuum simulations at the same time. In Figure 5, we show the differences between the discrete and continuum simulations at the same time. The network simulations agree to a remarkable extent with the PDE simulation, and also remarkably, the agreement begins very quickly in the evolution.

Recall that we used an approximation for f involving *instantaneous* queue length instead of mean queue length in (2). This approximation is justified if the variance of the instantaneous queue length is small relative to the mean queue length. Motivated by this observation, we conducted an experiment to measure the covariance between a node (i,j) and the queues at the

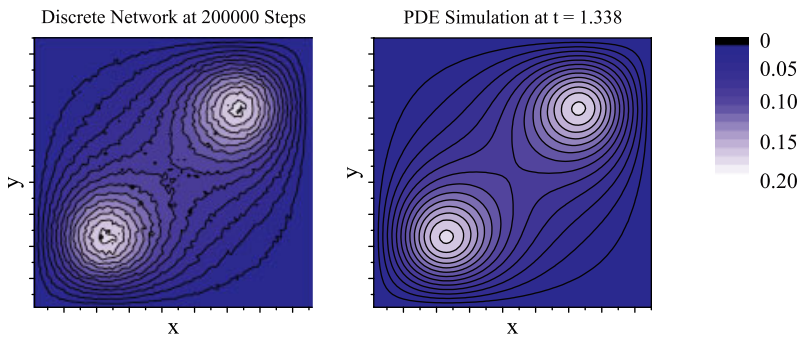

Figure 4. Contour plots of the normalized queue lengths for the discrete simulation with 83×83 nodes (left) and the PDE solution (right).

DOI: 10.1002/jnm

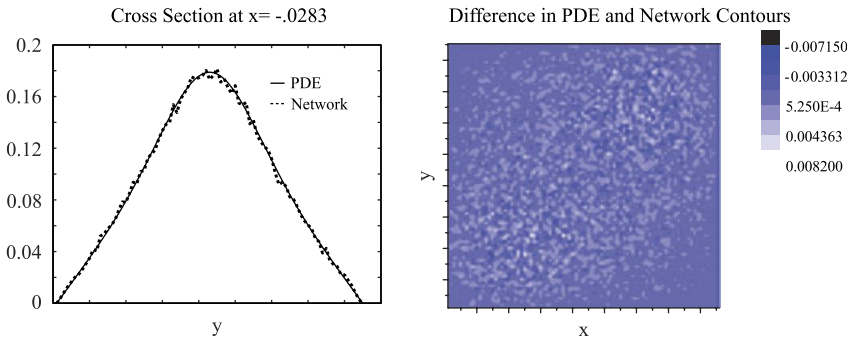

Figure 5. Cross-section plot of the normalized queue lengths for the discrete and PDE simulations (left) and a contour plot of the difference between the network state and the PDE solution (right).

nodes in the 5 node by 5 node grid centered at (i,j). We computed this matrix at all of the internal nodes at each time step in the discrete computation. A representative result is given by the following matrix, where the entries are given by the square root of the absolute values of the entries of the covariance matrix at the center point at a time that is halfway along the steady-state solution:

$$\begin{pmatrix} 0.6063 & 0.7473 & 0.6607 & 0.7834 & 0.6400 \\ 1.0742 & 0.0447 & 1.5191 & 0.9781 & 0.6871 \\ 1.2749 & 1.5841 & 3.9382 & 1.0530 & 0.8603 \\ 0.8264 & 0.5596 & 1.1322 & 1.1470 & 1.1575 \\ 0.8221 & 0.8466 & 0.9254 & 0.4035 & 0.9994 \end{pmatrix} \times 10^{-2}$$

Relative to the size of the queue, the covariances are small. In particular, the standard deviation of the instantaneous queue length (which is the quantity in the middle of the matrix) is approximately 0.04, which is an order of magnitude less than the mean queue length.

5. USING THE PDE MODEL

In this section, we demonstrate some of the possibilities enabled by the use of PDE models for the discrete networks. As pointed out above, direct computer simulation is currently the primary approach for performance analysis of networks. However, a serious barrier facing the use of direct simulation for evaluating the behavior of large networks is the prohibitive simulation time required to carry out the necessary Monte Carlo computations. The capability of computing accurate numerical solutions of PDE models using a tiny fraction of the time required to run a single network simulation raises the possibility of performance analysis and prototyping with a reasonable computational burden regardless of the size of the network being considered.

To illustrate the computational advantages arising from continuum modeling, we consider a network that has three highly localized sources, see Figure 6. The boundaries are mainly wall conditions, with three relatively small sink conditions placed at three locations. We also put a

DOI: 10.1002/jnm

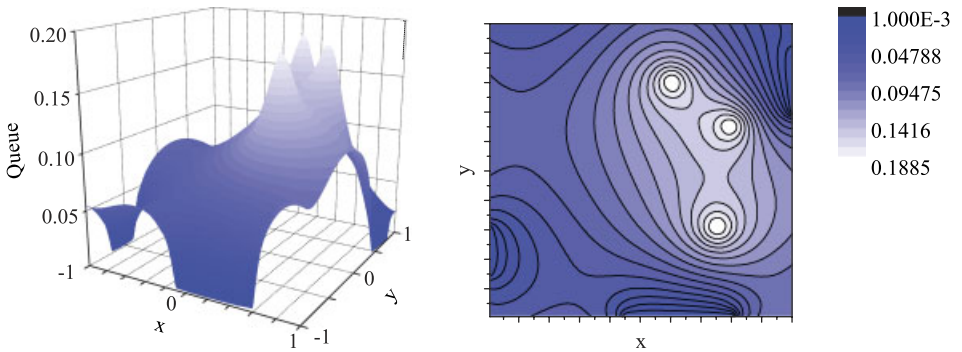

Figure 6. A steady-state, limiting behavior solution of the PDE model with three highly localized sources and three small regions of sink on the boundary. The sinks are indicated on the boundary of the domain. Left: surface plot. Right: contour plot.

mild constant convection away from the sources toward a far corner. The main point here is that it appears impossible to simulate the corresponding discrete network directly because of the density of nodes that would be required to represent the localized sources accurately. We can easily obtain a steady-state solution of the PDE simply by solving the problem for a sufficiently long time.

5.1. Analysis and comparison of network designs

We can use the PDE models to evaluate and compare multiple network design alternatives by comparing gross characteristics of network behavior, such as average delay and achievable throughput. Design issues amenable to evaluation by using the PDE models include network configuration and topology (including location of receivers, spatial density of nodes, and degree of connectivity of nodes), routing schemes, and network access protocols. Thus, modeling large networks using PDEs creates a powerful tool for *network design* and prototyping for very large networks.

5.1.1. Varying convection. In the first illustration, we compare steady-state (limiting behavior) PDE solutions corresponding to the same source and boundary conditions, but for which there are different convection coefficients. In the solution on the right in Figure 7, the convection is in the direction of front right-hand side to the back left-hand side. In the solution on the left, the convection is increased and runs diagonally from the right-hand corner to the left-hand corner. We can see that increasing the convection and changing the direction so as to point to an area located away from the source results in a relatively large region with an elevated queue size while the maximum height is smaller.

5.1.2. Varying boundary conditions. In the second example, we compare the steady-state (limiting behavior) solutions of the PDE model with the same load and convection coefficients but for which the boundary conditions are different. In the plot on the middle of Figure 8, we observe that the queue size near the corner where the walls meet is elevated compared with the solution with sink conditions on all four walls because signals find it difficult to leave that

DOI: 10.1002/jnm

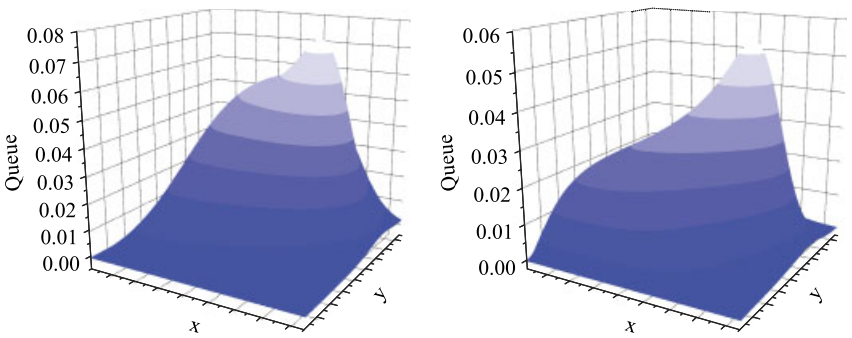

Figure 7. PDE solutions with different convection coefficients. Both solutions have convection in the x direction, whereas the solution on the right has additional convection in the y direction. All four boundaries are sinks.

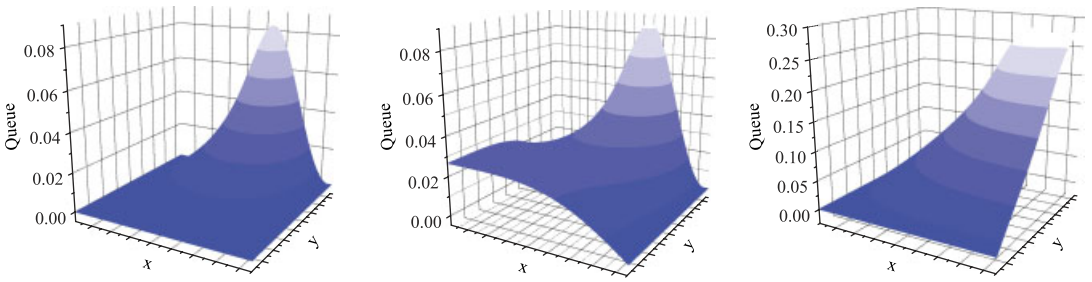

Figure 8. PDE solutions corresponding to different boundary conditions. The solution on the left has sink conditions on all four boundaries. The solution in the middle has a wall at the far boundary and sinks at the other three. The solution on the right has wall conditions on the wall next to the source and sinks on the other three.

region. In the plot on the right, we see that placing a source near walls drives the largest queue size up significantly.

5.1.3. Using convection to improve throughput. In this example, we measure the effects of varying convection on the throughput. The (normalized) instantaneous throughput at time t of the continuum model is given by

$$-\int_{\Omega}\left(\frac{\partial q(t,x,y)}{\partial t}-g(x,y)\right)\mathrm{d}x\,\mathrm{d}y \tag{7}$$

where Ω is the domain and g is the load. If q tends to a steady-state profile, then $\partial q/\partial t \to 0$ and the throughput will converge to the total input provided by the source. A positive throughput means that the solution is still increasing and there are signals in the network that have a finite probability of not reaching the receivers. In general, network designs that decrease the time it takes for the throughput to converge to the total input of the source are better.

DOI: 10.1002/jnm

To illustrate, we consider a network posed on the same domain with the same localized sink conditions as that shown in Figure 6. We place one relatively large source in the center of the domain. We show the different time plots corresponding to different size convection coefficients, where the convection is always pointed into the same corner of the domain, in Figure 9. In the plot on the left in Figure 9, we see that, up to a point, as we increase the size of the convection, the time taken for the throughput to converge to the maximum value decreases. However, as we increase the convection further, the time to convergence also begins to increase. This is illustrated in the plot on the right.

We show three of the steady-state profiles in Figure 10.

5.2. *Optimization of network characteristics*

The ability to evaluate networks quickly suggests that we can use the PDE models to solve network optimization problems (e.g. using the methods in [8]). The kinds of characteristics that arise and that are reflected naturally in continuum models include routing and other protocol parameters, flow rates, critical load levels, location of receivers, and so on. The corresponding control variables in the optimization problems for a PDE model include the form of the coefficients and parameters in those coefficients and location of the receivers on the boundaries.

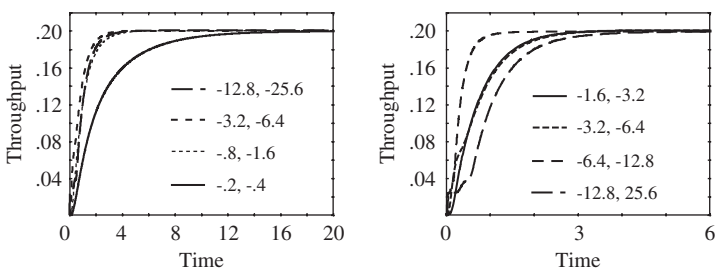

Figure 9. Plots of the throughput histories corresponding to different size convections. The values of $c_w - c_e$ and $c_n - c_s$ are used to label each curve. Right: plots over $[0, 20]$. Left: plots over $[0, 6]$.

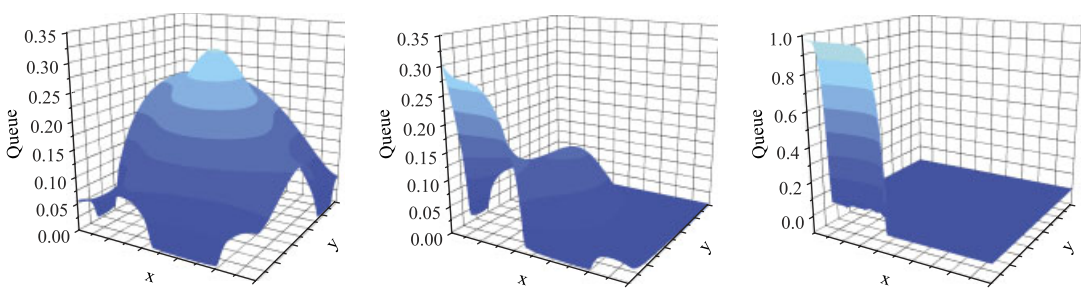

Figure 10. PDE solutions corresponding to varying convection coefficients. Note that a very large convection, shown on the right, leads to near instability with the queue size reaching the physically meaningful limit. Any further increase leads to unbounded growth in the queue.

DOI: 10.1002/jnm

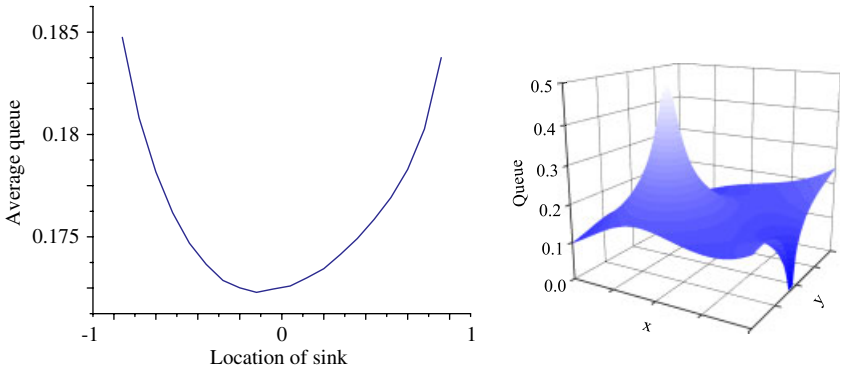

Figure 11. Left: plot of the average queue size versus location of the sink. Right: plot of the optimal queue distribution.

Several meaningful performance metrics are possible. First, it may be of interest to minimize the steady-state queue length averaged over the nodes. This also minimizes the steady-state delay. Second, we may be interested in 'load balancing' over the network, in which case the optimization problem is to minimize the spread in the queue lengths over the network. Third, we may constrain the steady-state average queue length and maximize the achievable throughput subject to this constraint. Finally, instead of steady-state quantities, we may be interested in transient versions of these quantities, such as a time average over some finite initial time horizon.

To illustrate, we consider the following optimization problem. We pose the PDE model (6) with the conditions

$$g(x,y) = 0.2 \times \mathrm{e}^{-100((x+0.3)^2+(y+0.3)^2)}/0.03141593$$

$$c_{\mathrm{w}} - c_{\mathrm{e}} = -0.5, \quad c_{\mathrm{s}} - c_{\mathrm{n}} = -0.2$$

and initial condition 0 on the domain $[-1,1] \times [-1,1]$. For boundary conditions, we use wall conditions on all the boundaries, except for sink condition posed on a small piece of size 0.1 located along the boundary away from the source in the direction of the convection. The optimization problem is to find the position of the sink to minimize the average queue size over the domain at time $t = 4$, which represents several hundred thousand discrete time steps in a network of reasonable size (the number of steps is obtained from the formula $t = k\,\mathrm{d}t/Q_{\max}$). In Figure 11, we show the results. There is a clear minimum found quickly and easily using the PDE model.

6. CONCLUSIONS AND FUTURE WORK

In this paper, we develop a mathematical approach for modeling extremely large networks using time-dependent partial differential equations (PDEs) based on taking an asymptotic limit of a stochastic description of communication in the network. Using a number of examples, we demonstrate that the PDE models capture global characteristics of the networks with remarkable accuracy. We also demonstrate that the PDE models provide a powerful way to deal with the number of components in large networks. This makes it possible to carry out—with reasonable computational burden even for very large systems—network performance evaluation and prototyping, network design, systematic parameter studies, and optimization of network characteristics.

DOI: 10.1002/jnm

The use of PDE models to simulate large networks opens up enormous possibilities for network performance evaluation and prototyping, network design, systematic parameter studies, optimization of network characteristics, and solving network inverse problems. We will consider these applications in future work.

REFERENCES

1. Gupta P, Kumar P. The capacity of wireless networks. *IEEE Transactions on Information Theory* 2000; **IT-46**: 388–404.
2. Grossglauser M, Tse D. Mobility increases the capacity of adhoc wireless networks. *IEEE/ACM Transactions on Networking* 2002; **10**:477–486.
3. Xie L-L, Kumar PR. A network information theory for wireless communication: scaling laws and optimal operation theory for wireless communication: scaling laws and optimal operation. *IEEE Transactions on Information Theory* 2004; **50**:748–767.
4. Herdtner J, Chong EKP. Throughput-storage tradeoff in *ad hoc* networks. *Proceedings of the 2005 IEEE INFOCOM*, Miami, Florida, March 2005.
5. *DASensors and Sensor Networks Program Solicitation NSF 03-512*. http://www.nsf.gov/pubs/2003/nsf03512/nsf03512.htm
6. Gastpar M, Vetterli M. Scaling laws for homogeneous sensor networks. *Forty-First Annual Allerton Conference on Communication, Control and Computers*, Monticello, IL, 2003.
7. Gamal HE. On the scaling laws of dense wireless sensor networks: The data gathering channel. *IEEE Transactions on Information Theory*, 2005; **51**(3):1229–1234.
8. Chong EKP, Zak SH. *An Introduction to Optimization* (2nd edn). Wiley: New York, NY, 2001.

AUTHORS' BIOGRAPHIES

Edwin K. P. Chong received the BE(Hons.) degree with First Class Honors from the University of Adelaide, South Australia, in 1987; and the MA and PhD degrees in 1989 and 1991, respectively, both from Princeton University, where he held an IBM Fellowship. He joined the School of Electrical and Computer Engineering at Purdue University in 1991, where he was named a University Faculty Scholar in 1999, and was promoted to Professor in 2001. Since August 2001, he has been a Professor of Electrical and Computer Engineering and a Professor of Mathematics at Colorado State University. His current interests are in communication networks and optimization methods. He coauthored the recent best-selling book, *An Introduction to Optimization*, 2nd Edition, Wiley-Interscience, 2001. He was on the editorial board of the IEEE Transactions on Automatic Control, and is currently an editor for Computer Networks and the Journal of Control Science and Engineering. He is a Fellow of the IEEE, and served as an IEEE Control Systems Society Distinguished Lecturer. He received the NSF CAREER Award in 1995 and the ASEE Frederick Emmons Terman Award in 1998. He was a co-recipient of the 2004 Best Paper Award for a paper in the journal *Computer Networks*. He has served as Principal Investigator for numerous funded projects from DARPA and other defense funding agencies.

Donald Estep received a BA from Columbia University in 1981 and MS and PhD degrees in applied mathematics from the University of Michigan in 1987. From 1987 to 2000, he worked in the School of Mathematics at the Georgia Institute of Technology, where he was promoted to Professor. Joining the faculty at Colorado State University in 2000, he is a Professor in the Departments of Mathematics and of Statistics. Dr Estep works in numerical analysis, scientific computing, applied analysis, and uncertainty analysis for multiscale, multiphysics models. During 1993–1995, he was a National Science Foundation International Research Fellow. During 1991–1993, he was a visiting assistant professor in Applied Mathematics at the California Institute of Technology. He was awarded the Computational and

DOI: 10.1002/jnm

Mathematical Methods in Sciences and Engineering Prize in 2005. Currently, he is a principal or co-principal investigator on multiple projects funded by the DOE, NASA, NSF, and the USDA. Dr Estep is the co-director of the Program for Interdisciplinary Mathematics, Ecology, and Statistics, an NSF IGERT program. He is co-author of several undergraduate and graduate textbooks in analysis and numerical analysis. He was awarded the Outstanding Professor in Graduate Instruction in Mathematics in 2005 and the College of Natural Sciences Award for Excellence in Graduate Education and Mentoring in 2007. Dr Estep is on the editorial board of the *SIAM Journal on Numerical Analysis* and on the SIAM Education Committee.

Jan Hannig received the Mgr (MS equivalent) degree in Mathematics from Charles University, Prague, Czech Republic, in 1996; and the PhD degree in Statistics from Michigan State University, in 2000. He is currently an Associate Professor in the Department of Statistics, Colorado State University. His research interests are in probability and theoretical statistics.

DOI: 10.1002/jnm